15TH IEA HEAT PUMP CONFERENCE
MAY 26–29, 2026 | HOFBURG
VIENNA 2026
DECARBONISATION THROUGH INNOVATION

Construction of transfer functions for standing column wells operating with bleed

Christopher Rose[a,*], Philippe Pasquier[a], Alain Nguyen[b], Richard Labib[a]

[a]Polytechnique Montréal, P.O. Box 6079 Station Centre-Ville, Montréal, H3C 3A7, Canada
[b]Natural Resources Canada, 1615 Lionel-Boulet, P.O. Box 4800, Varennes, J3X 1S6, Canada

Abstract

Standing column wells (SCW) offer a cost-effective and space-efficient alternative to conventional closed-loop ground heat exchangers, making them particularly suited for urban environments and retrofit applications. By recirculating groundwater within a deep uncased borehole and discharging a controlled fraction during peak loads, a process known as "bleed", SCWs take advantage of advective heat transfer to enhance the system's performance. However, the design of SCW systems remains challenging due to the absence of simulation tools capable of simultaneously accounting for both hydraulic and thermal interactions between SCWs operating with bleed. This study presents a modelling framework for constructing transfer functions for fields of SCWs connected in parallel. The method combines numerically simulated thermal responses of an individual borehole and pairwise thermal interactions between SCWs with the successive flux algorithm, enforcing uniform inlet temperature boundary conditions. When bleed is active, all SCWs in the ground heat exchanger are explicitly modelled to accurately reproduce the groundwater velocity field and its influence on advective heat transfer. The method is verified against a large-scale 3D finite element model representing six SCWs located in a stratified and fractured aquifer and operating under different flow rate scenarios. Results show strong agreement with the reference simulations when the groundwater velocity field of the complete ground heat exchanger is represented. In contrast, modelling only two SCWs at a time yields accurate results solely in the absence of bleed.

Keywords: Ground-source heat pump; Ground heat exchanger; Standing column well; Thermal interaction; Transfer function; g-function

1. Introduction

Ground-source heat pump systems are increasingly deployed worldwide, as they offer efficient and sustainable means to cover the thermal needs of buildings, while also reducing greenhouse gas emissions and operating costs over time [1]. Among ground heat exchangers (GHE), which consist of one or more boreholes, standing column wells (SCW) provide a cost-effective alternative to conventional closed-loop systems [2-4], requiring fewer boreholes and less materials (i.e., no grout, no antifreeze, reduced vertical and horizontal piping). In a SCW, groundwater is mainly recirculated within a deep, uncased borehole. During periods of peak power demands, a fraction of the pumped groundwater may be discharged to an injection well, sewer, surface water body, or reintroduced through inter-well reinjection [5-6]. This process, known as "bleed", induces a drawdown within the SCW, promoting convergent groundwater flow, thereby enhancing advective heat transfer and renewing the groundwater in the borehole. As a result, bleed helps stabilize the heat pump's inlet temperature, notably under unbalanced thermal loads, and can temporarily boost the system's thermal efficiency [7]. SCWs also exhibit significant thermal inertia owing to the large volume of groundwater contained within the borehole and they benefit from long fluid residence time, both of which help to dampen peak loads [8]. These characteristics make SCWs a compelling option, ideal for use in space-constrained urban settings and retrofit projects [9-10], particularly in regions facing power and energy supply constraints.

* Corresponding author.
E-mail address: christopher.rose@etud.polymtl.ca

Nevertheless, the design of SCWs remains challenging because of the scarcity of efficient and user-friendly simulation tools.

Recent studies have focused on improving the design methodologies of SCWs. Dion and Pasquier [4] proposed new sizing equations, analogous to the alternative ASHRAE approach for closed-loop boreholes [11], emphasizing the need for hourly simulations to ensure compliance with heat pump's operating temperature limits. However, the method used assumes constant operating conditions and bleed has not yet been fully integrated into the analytic formulation. The dynamic control of pumping and bleed flow rates has been demonstrated to achieve a balanced compromise between thermal performance and reduced groundwater discharge in comparison with constant operations [12-13]. In this context, Beaudry et al. [14] introduced a dynamic simulation framework based on non-stationary convolution [15-16] with the aim of minimizing energy consumption, power demand, operating cost, and groundwater usage. The analysis indicated that maintaining an approximate 2 °C temperature difference across the heat pump results in operating conditions that are close to optimal. From the simplified sizing equations of Dion and Pasquier [4] to the more advanced dynamic control scheme of Beaudry et al. [14], both design methods share a common limitation in that they rely on transfer functions obtained with complex and computationally intensive numerical models.

Traditionally, g-functions are used to describe the GHE's thermal response to a constant impulse through a smooth monotonic transfer function representing the evolution of the mean borehole wall temperature [17]. Alternatively, transfer functions can be defined in terms of the borehole outlet fluid temperature [18], directly capturing the heat transfer between the circulating fluid and the surrounding ground, while already accounting for short-term effects arising from borehole thermal capacities and fluid residence time. In contrast to classical g-functions, which assume a uniform borehole wall temperature along and between boreholes in the GHE, transfer functions allow both the heat flux and the borehole wall temperature to vary spatially, thereby providing a more realistic boundary condition [19]. The construction of a transfer function involves the simulation of two distinct elements: (1) the thermal response of an individual borehole and (2) the pairwise thermal interactions among boreholes within the GHE [20].

The construction of transfer functions for SCWs is a particularly challenging endeavour due to the necessity of solving the governing advection-diffusion equation, a task that is typically achieved through the use of numerical models [8]. While these numerical models have been validated experimentally for a single borehole through thermal response tests, pumping tests, and operational data [21-23], their runtime and memory requirements still pose a limitation [8]. The classical line-source approaches (i.e., moving, finite or infinite line source models) are unsuccessful under bleed conditions. To overcome this limitation, Nguyen et al. [24] developed an analytical model for a single SCW in a homogeneous aquifer by scaling the infinite line source solution with a radial convergence term. Jacques et al. [25] extended this model to account for layered heterogeneity and for different pumping and reinjection depths. In a recent study, Rose et al. [26] trained an artificial neural network to predict the short-term transfer functions of a SCW within milliseconds, providing a fast surrogate model trained on a finite element model (FEM) similar to that of Beaudry et al. [22]. Despite the existence of a limited number of modelling strategies for a single SCW [24], simulating an entire field of SCWs still requires the use of large-scale 3D numerical models [25] which impose significant computational time and memory requirements. This, in turn, limits their practicality for routine design and restricts the number of boreholes that can be simulated. To the best of the authors' knowledge, no existing method allows for the simulation of pairwise thermal interactions between SCWs.

In their recent study, Rose et al. [27] introduced a modelling strategy for closed-loop GHEs connected in parallel, capable of reproducing transfer functions obtained from large-scale 3D numerical models across timescales from seconds to years. The method consists of a series of numerical simulations involving two complete boreholes, one of which acts as an emitter and the other as a receiver. The thermal response of an individual borehole is evaluated at the emitter's outlet, while the pairwise thermal interaction is measured at the receiver's outlet. In order to ensure uniform inlet fluid temperatures across all boreholes, the authors implemented the block-matrix algorithm of Dusseault et al. [28]. This unified framework inherently accounts for vertical variations in both heat flux and borehole wall temperature along and between boreholes, offering a more realistic representation of parallel-connected systems. The use of numerical simulations allows the implicit inclusion of groundwater flow and geological heterogeneity, which are key factors governing the thermal behaviour of SCWs [22-23].

The present study builds on the foundation laid by Rose et al. [27] with respect to SCWs. The method integrates numerically simulated thermal interactions between SCWs with the successive flux algorithm of Nguyen and Pasquier [29], enforcing boundary conditions of uniform inlet temperatures. The proposed framework is verified against reference numerical solutions under various operating scenarios.

2. Methodology

This section presents the methodology used to construct transfer functions for a field composed of several SCWs interacting hydraulically and thermally with one another. Section 2.1 provides a brief overview of the overall approach and discusses the specific modelling considerations associated with SCWs operating under bleed conditions, while Section 2.2 details the numerical model used to simulate the thermal interactions between SCWs.

2.1. Overview of the method

As previously stated, the construction of a transfer function requires simulating both the thermal response of an individual borehole and the pairwise thermal interactions among boreholes within the GHE [20]. The approach of Rose et al. [27] for simulating thermal interactions between boreholes can be directly extended to SCWs operating in full recirculation mode (i.e., without bleed). Accordingly, each unique thermal interaction, defined by a specific borehole spacing, is obtained by numerically simulating two SCWs separated by that radial distance. In each simulation, two SCWs are modelled, with one acting as the emitter and the other as the receiver. The emitter borehole is subjected to a constant unit temperature impulse between its inlet and outlet ($T_{\text{in}}(t) - T_{\text{out}}(t) = 1$ °C), while the receiver borehole operates under identical operating conditions, but without a thermal impulse ($T_{\text{in}}(t) - T_{\text{out}}(t) = 0$). This setup yields two response functions: (1) the thermal response of an individual borehole, measured at the emitter's outlet, and (2) the pairwise thermal interaction, measured at the receiver's outlet. Fig. 1 illustrates this modelling strategy for a pair of SCWs distanced by a radial distance of $r_{1,3}$, where SCW #1 acts as the emitter and SCW #3 as the receiver, within a field of six SCWs.

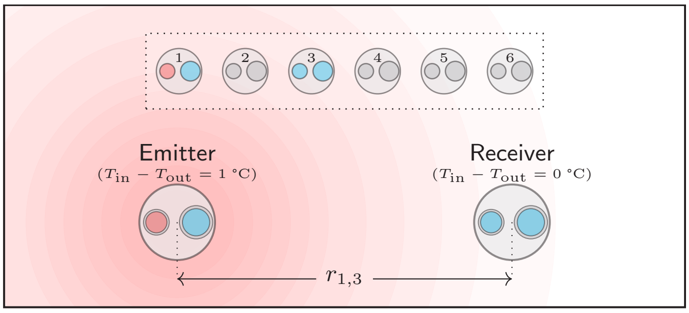

Figure 1. Illustration of the modelling strategy with two standing column wells operating without bleed. The configuration represents the thermal interaction between the emitter borehole (#1) and the receiver borehole (#3), separated by a radial distance $r_{1,3}$. Warmer temperatures are shown in red. The smaller-diameter pipe corresponds to the injection pipe, while the larger one represents the riser pipe equipped with a submersible pump.

However, when bleed is activated, the approach of Rose et al. [27] can no longer be directly extended to SCWs. Modelling only two SCWs at a time to simulate thermal interactions among boreholes introduces a limitation in the representation of the groundwater velocity field. As previously stated, discharging a fraction of the pumped groundwater outside the SCW induces a drawdown within the well and the surrounding aquifer. Since hydraulically connected SCWs influence one another, drawdowns, and therefore the resulting velocity field, are affected by neighbouring wells. Consequently, the velocity field simulated when only two SCWs are modelled differs from that obtained when all SCWs in the GHE are represented, leading to an inaccurate estimation of the advective heat transfer component. Fig. 2 compares the scaled drawdowns computed using the Theis equation [30] for two (left) and six (right) SCWs operating with bleed. Note that both maps use the same scale and that the drawdown distribution differs markedly when multiple SCWs are modelled. To properly perform spatial superposition of heat sources, the simulated groundwater velocity field must reproduce that of the GHE. Therefore, when SCWs operate under bleed conditions, each SCW in the GHE is modelled, with one acting as the emitter while the others serve as receivers. Sections 3.2 and 3.3 further demonstrate the importance of accurately representing the velocity field for spatial superposition.

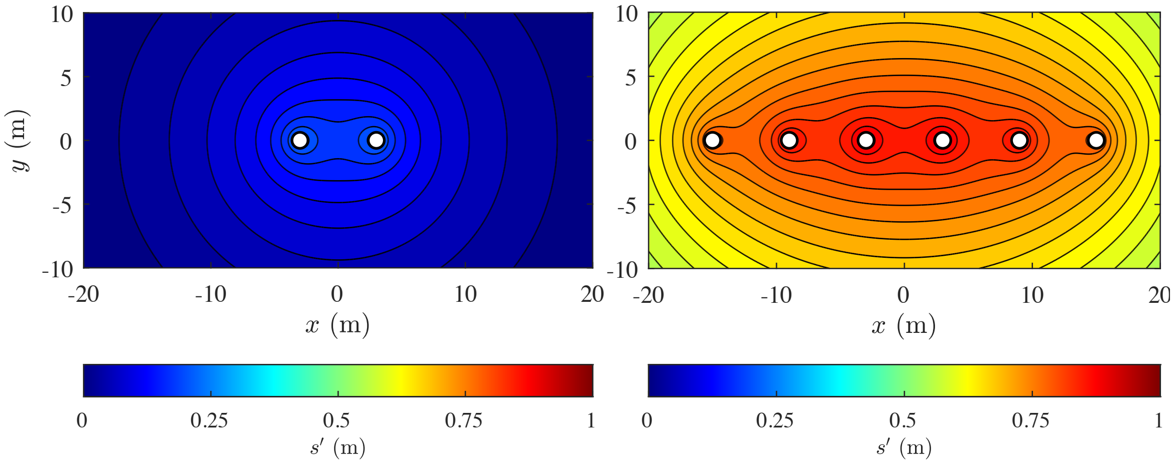

Figure 2. Comparison of normalized drawdowns computed using the Theis equation [30] for two (left) and six (right) standing column wells operating under bleed conditions. Both maps use the same scale, and white circles indicate the borehole locations.

Once every unique pairwise thermal interaction and the thermal response of an individual borehole have been simulated using the modelling strategy detailed in Section 2.2, spatial superposition can be performed. Several methods have been proposed to perform spatial superposition and enforce uniform temperatures across boreholes [20,28-29,31,32]. Among these, the successive flux algorithm of Nguyen and Pasquier [29] is certainly one of the most efficient algorithms. Essentially, this algorithm iteratively adjusts the heating power of each borehole at every time step to ensure that they all maintain the same prescribed temperature. In this study, this prescribed temperature corresponds to a uniform inlet temperature. Since boreholes thermally interact with each other and disturb the surrounding ground temperature to varying degrees, the inlet temperature must dynamically adjust over time to reflect the location of a given SCW within the GHE. Ultimately, spatial superposition yields a transfer function that describes the GHE's thermal response to a unit impulse. Readers are referred to the work of Nguyen and Pasquier [29] for additional details.

2.2. Finite element model

Every SCW in the GHE, located within a multilayered and fractured aquifer, are modelled in COMSOL Multiphysics (v. 6.0) through a 3D FEM coupling groundwater flow and heat transfer. The modelling strategy builds upon the previous study of Beaudry et al. [14], where SCWs are represented in an up-pump configuration and the larger diameter of the pumping chamber is neglected. The properties of the groundwater are fixed at a reference temperature of 10 ˚C, as to ensure a linear and time-invariant system [15-16]. Thus, hydraulic conductivity is not temperature dependent and both viscosity and density of groundwater remain constant.

Following the recommendations of Rose et al. [27] on meshing, the horizontal element size was limited to 0.5 m between the SCWs to prevent numerical inaccuracies arising from mesh coarsening away from the heat source. A triangular surface mesh was generated and subsequently extruded along the vertical direction according to the thickness of each geological layer. As customary, a mesh independence analysis was conducted to ensure numerical accuracy and stability of the solution.

2.2.1. Governing equations

The transient heat transfer is described by the energy conservation equation, solved in all domains ($\boldsymbol{\Omega}$) using the finite element method:

$$(\rho c)_{eq}\frac{\partial T}{\partial t} + (\rho c)_w \boldsymbol{u}\cdot\nabla T = k_{eq}\nabla^2 T \quad (x,y,z) \in (\boldsymbol{\Omega}) \tag{1}$$

where k and ρc are respectively the thermal conductivity and the volumetric heat capacity, subscripts eq and w refer to the equivalent properties of the porous medium and the groundwater, $\boldsymbol{u}$ is a fluid flow vector and T is the temperature within the domain delimited by the boundary conditions illustrated in Fig. 3 and discussed in Section 2.2.2.

The equivalent thermal properties of the bedrock matrix are expressed as an equivalent homogeneous and isotropic porous medium:

$$\phi_{eq} = (1-n)\phi_s + n\phi_f \tag{2}$$

where ϕ represents either the thermal conductivity (k) or the volumetric heat capacity (ρc), n is the porosity, and subscripts s and f denote the solid and fluid phases, respectively.

The fluid flow vector corresponds to Darcy's apparent velocity field:

$$\boldsymbol{u} = -K \cdot \nabla h \tag{3}$$

where K is the hydraulic conductivity tensor and h is the hydraulic head, which is obtained by solving the mass continuity equation for a saturated medium without a source term:

$$S_s \frac{\partial h}{\partial t} = \nabla \cdot (K \cdot \nabla h) \tag{4}$$

where S_s is the specific storage of the porous medium.

Productive fractures are represented as 2D horizontal planes of prescribed aperture and are assumed to be fully open. Groundwater flow and associated heat transfer along these fractures are computed using the tangential derivatives of Darcy's law and the heat fluxes, following the approach used by Champagne-Péladeau et al. [33].

2.2.2. Initial and boundary conditions

Fig. 3 illustrates the boundary conditions applied in the numerical model, along with the different domains, namely the groundwater, the fractured aquifer and the pipes, assuming a GHE composed of two SCWs. The initial conditions, given by Eqs. (5 – 6), define the hydraulic and thermal states prior to the application of the thermal impulse and the operating flow rates. The initial hydraulic head is set to a constant value H throughout the domains ($\boldsymbol{\Omega}$), corresponding to the sum of the saturated length of the SCW and the underlying bedrock. This ensures a fully saturated aquifer at hydrostatic equilibrium:

$$h(t=0) = H \quad (x,y,z) \in (\boldsymbol{\Omega}). \tag{5}$$

The initial temperature field is assumed to be uniform and equal to zero in all domains:

$$T(t=0) = 0 \quad (x,y,z) \in (\boldsymbol{\Omega}). \tag{6}$$

These initial conditions ensure that any subsequent temperature variations arise solely from the imposed unit impulse at the emitter borehole and the resulting coupled groundwater flow and heat transfer processes.

For both SCWs, the hydraulic boundary conditions specify the imposed volumetric flow rates. At the borehole outlets (Γ_2 and Γ_4), a pumping rate ($\dot{V}$) is prescribed, while at the borehole inlets (Γ_1 and Γ_3), the inflow equals to the pumping flow rate minus the bleed flow rate ($\dot{B} = \beta\dot{V}$):

$$-\boldsymbol{n} \cdot \boldsymbol{u} = \frac{\dot{V}(1-\beta)}{A_{in}} \quad (x,y,z) \in (\Gamma_1, \Gamma_3) \tag{7}$$

$$-\boldsymbol{n} \cdot \boldsymbol{u} = \frac{-\dot{V}}{A_{in}} \quad (x,y,z) \in (\Gamma_2, \Gamma_4) \tag{8}$$

where β is the bleed ratio, A_{in} is the internal cross-sectional area of both the riser and reinjection pipes, and $\boldsymbol{n}$ is the unit vector perpendicular to the boundary.

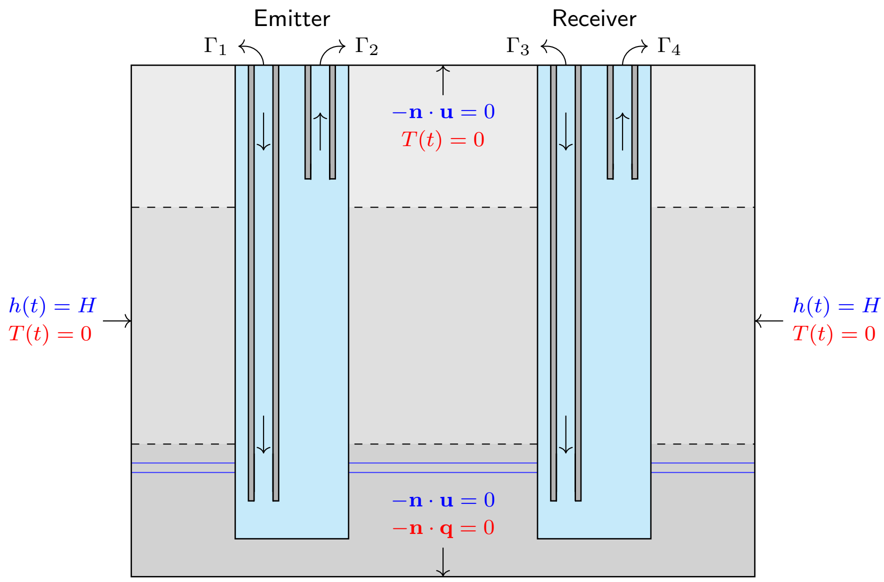

Figure 3. Boundary conditions (**Γ**) of the finite element model for a field composed of two standing column wells. Lateral boundaries are assigned a zero-temperature condition and a constant hydraulic head, assuming the absence of regional groundwater flow. The top and bottom boundaries are treated as zero-flux for groundwater flow. A zero geothermal heat flux is prescribed at the model base, while the surface is maintained at a constant zero-temperature. Grayscale shading represents the layered aquifer, and blue lines indicate productive fractures modelled as 2D horizontal planes. Refer to Eqs. (7 – 11) for the remaining boundary conditions.

The thermal boundary conditions are defined by Eqs. (9 – 11). A prescribed temperature is assigned to the emitter's borehole inlet (Γ_1), corresponding to the outlet temperature (T_{out}) plus a unit temperature impulse:

$$T_{in}(t) = T_{out}(t) + 1 \quad (x, y, z) \in (\Gamma_1). \tag{9}$$

The receiver's borehole inlet (Γ_3) is maintained at the corresponding outlet temperature:

$$T_{in}(t) = T_{out}(t) \quad (x, y, z) \in (\Gamma_3). \tag{10}$$

Finally, the borehole outlet of both SCWs (Γ_2 and Γ_4) are defined as an open boundary condition:

$$-\boldsymbol{n} \cdot (\rho c)_w \left(\boldsymbol{u} \cdot \frac{\partial T}{\partial z}\right) = \boldsymbol{q}_c \quad (x, y, z) \in (\Gamma_2, \Gamma_4) \tag{11}$$

where $\boldsymbol{q}_c$ is the outflow convective heat flux vector.

3. Results and discussion

The proposed methodology is verified in this section by comparing the constructed transfer functions with those obtained from a large-scale 3D numerical model that fully represents the parallel-connected GHE, which serves as the reference FEM. The comparison is first performed for the approach where the velocity field matches that of the GHE, followed by the approach in which only two SCWs are modelled at a time.

3.1. Comparative scenario

The selected scenario is inspired by a real ongoing project involving 6 SCWs, that aims to supply approximately 1 MW of heating power in Montréal, Canada. Given the typical depth of SCWs, it is common to intersect multiple hydrogeological layers and fractured zones. To illustrate the approach developed in this work, a relatively complex geological model integrating layered heterogeneities and productive fractures was used. The depth of each SCW was selected to 500 m, and a small spacing between the SCWs was chosen to increase thermal interactions. Properties of the hydrogeological layers, the fractures and the pipe material are detailed in Table 1. Simulations were performed for an operating flow rate of 50 GPM (189 L/min), and for bleed ratios of 0 %, 5 %, 10 % and 20 %. The discharged groundwater is assumed to be directed towards a sewer system.

Table 1. Thermal and hydraulic properties of the hydrogeological environment, fully open productive fractures, and pipe material.

Properties	Layer 1	Layer 2	Layer 3	Fractures	Pipes
Thickness – b [m]	150	250	125	0.0025	–
Thermal conductivity – k [Wm^{-1}K^{-1}]	2.75	2.25	3.0	0.5761	0.4
Volumetric heat capacity – ρc [MJm^{-3}K^{-1}]	2.4	2.5	2.3	4.1976	2.3
Hydraulic conductivity – K [ms^{-1}]	10^{-8}	5×10^{-8}	10^{-7}	10^{-2}	–
Specific storage – S_s [m^{-1}]	5×10^{-5}	5×10^{-5}	5×10^{-5}	10^{3}	–
Porosity – n [–]	0.03	0.02	0.01	1	–

The layout of the GHE, along with a plan and sectional view of a SCW, is illustrated in Fig. 4. All SCWs in the GHE are assumed to be identical. As shown, the submersible pump is positioned 20 m below the static water level, while the sedimentation chamber at the bottom of the SCW has a fixed height of 10 m. The numerical model also includes an additional 25 m of bedrock beneath the SCWs. Grayscale shading distinguishes the three hydrogeological layers, while blue lines indicate the two productive fractures located at depths of 450 m and 475 m, which both share identical thickness and properties (see Table 1).

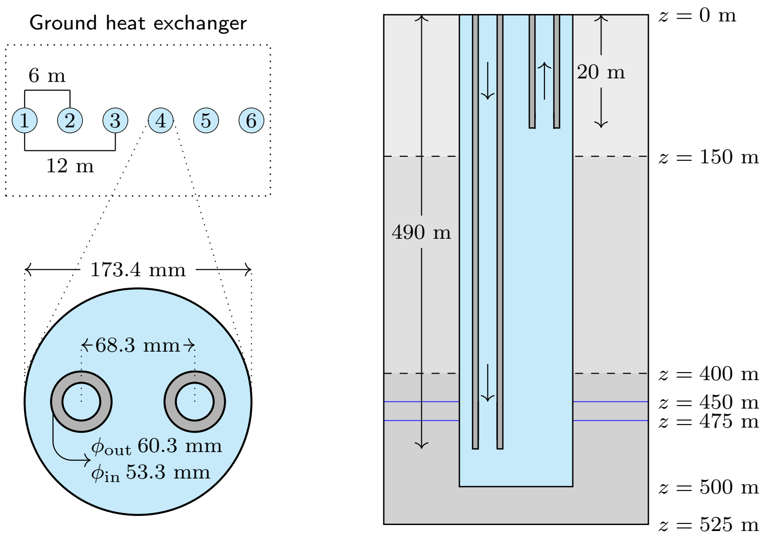

Figure 4. Illustration of the ground heat exchanger composed of six standing column wells, showing the geological stratigraphy (grayscale), the depths of the productive fractures (blue lines), and the geometry of the injection and riser pipes (not to scale).

3.2. Verification of the approach

Fig. 5 (left) compares the transfer functions obtained with the method described in Section 2, where all SCWs are modelled, with those from the reference numerical model for different bleed ratios (β). The proposed method shows strong agreement across all flow rate scenarios, as evidenced by the low relative root mean square error (RRMSE) and maximum relative error (MaxRe) values reported in Table 2. These results confirm that the method reliably reproduces the reference transfer functions under complex stratified hydrogeological conditions with fractured flow.

Fig. 5 (right) illustrates all pairwise thermal interactions among SCWs in the GHE for a bleed ratio of 20 %, color-coded by radial distance. Observe that the thermal interactions, for a given radial distance, are not unique and exhibit noticeable variability, particularly for a spacing of 6 m (yellow). To highlight this effect, two cases are shown in which the emitter (SCW #2) transfers heat to the receivers (SCW #1 and SCW #3), both located at the same radial distance from the emitter (see Fig. 4 for borehole numbering). The results show that the receiver positioned closer to the centre of the GHE (SCW #3) experiences a temperature increase up to approximately 8 % greater than that of the outer receiver (SCW #1). This difference arises because groundwater, and consequently heat, flows toward regions of lower hydraulic head (i.e., higher drawdown), that is, toward the centre of the GHE. One can refer to Fig. 2 that illustrates an example of the normalized drawdown field for a GHE composed of six SCWs.

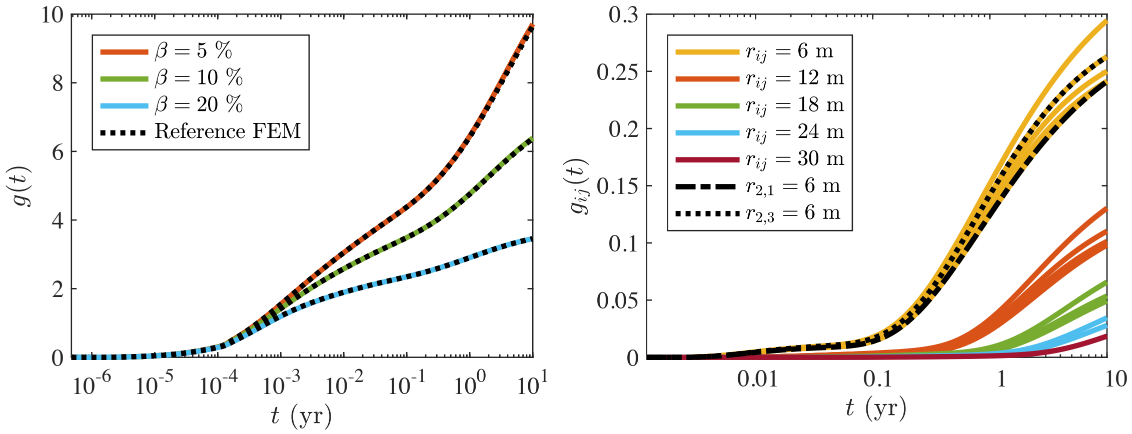

Figure 5. (Left) Transfer functions ($\boldsymbol{g}$) for the ground heat exchanger illustrated in Fig. 4 operating at various bleed ratios (β). Solid coloured lines correspond to the transfer functions constructed using the methodology described in Section 2, which explicitly accounts for the groundwater velocity field. Dotted lines denote the transfer functions obtained with the reference finite element model. (Right) Pairwise thermal interactions ($\boldsymbol{g}_{ij}$) within the ground heat exchanger used to construct the transfer function for the case with a 20 % bleed ratio.

3.3. Modelling two standing column wells

The direct extension of the approach of Rose et al. [27], where only two SCWs are modelled, shows strong agreement with the reference solutions only in the case without bleed (see Fig. 6, left), as indicated by the low RRMSE and MaxRe values in Table 2. These values corresponding to $\beta = 0$ % are of the same order of magnitude as those obtained when all SCWs are modelled with bleed. This outcome is expected, since without bleed activated, the groundwater velocity field surrounding the SCWs remains unaffected by their operation, similar to closed-loop boreholes. When bleed is activated, however, the method fails to reproduce the reference transfer functions accurately, particularly towards the end of the simulation. The discrepancies reach about two orders of magnitude higher in RRMSE than in the no-bleed case and about 9 % in MaxRe.

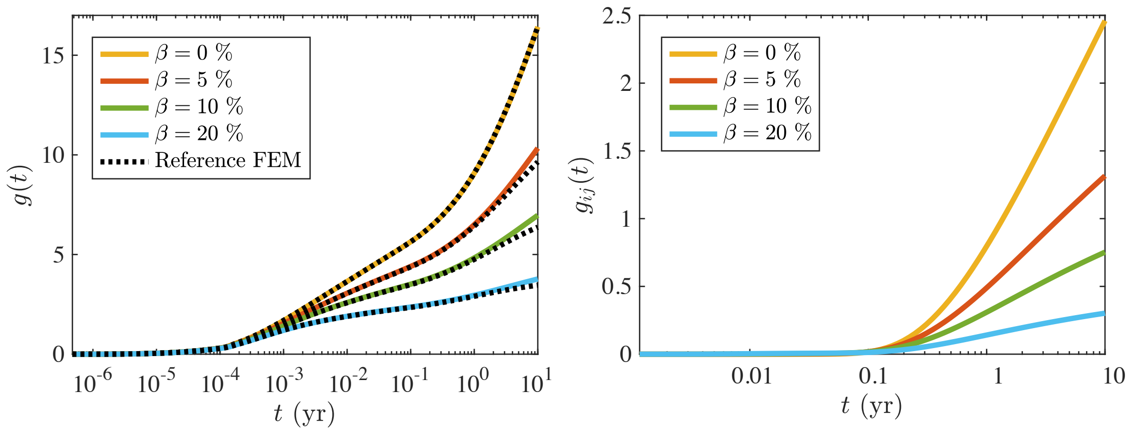

Figure 6. (Left) Transfer functions ($\boldsymbol{g}$) for the ground heat exchanger illustrated in Fig. 4 operating at various bleed ratios (β). Solid coloured lines correspond to the transfer functions constructed using the methodology described in Section 2, without explicitly accounting for the groundwater velocity field. Dotted lines denote the transfer functions obtained with the reference finite element model. (Right) Pairwise thermal interactions ($\boldsymbol{g}_{ij}$) between standing column wells for a fixed radial distance of 6 m under various bleed ratios.

Fig. 6 (right) shows the simulated thermal interactions between SCWs separated by a radial distance of 6 m for different bleed ratios. Increasing the bleed ratio reduces thermal interactions between boreholes, suggesting that SCWs could be positioned closer together when bleed is frequently activated, an important advantage for dense urban environments. However, unlike the modelling strategy where all SCWs are represented, the thermal interactions between boreholes separated by the same radial distance remain identical, regardless of the emitter or receiver's position within the GHE.

Table 2. Relative root mean square error (RRMSE) and maximum relative error (MaxRe) between transfer functions obtained with the approach outlined in Section 2, when all six SCWs are modelled and when only two SCWs are modelled, and those from the reference numerical model.

Bleed ratio (%)	Six SCWs (Fig. 5)		Two SCWs (Fig. 6)	
	RRMSE (%)	MaxRe (%)	RRMSE (%)	MaxRe (%)
0	–	–	8.07×10^{-5}	0.13
5	4.16×10^{-4}	0.69	2.95×10^{-3}	7.18
10	1.70×10^{-4}	0.30	3.63×10^{-3}	9.40
20	1.80×10^{-4}	0.27	3.25×10^{-3}	9.13

Simulations involving the complete GHE were computationally demanding and were therefore performed on a high-performance computing cluster, requiring up to 110 GB of memory and more than 7 h of wall-clock time. By comparison, simulations involving two SCWs required up to 50 GB of RAM and an average runtime of approximately 4 h when executed on a workstation equipped with an Intel Core i9-12900KF 3.20 GHz 16-core processor.

The key takeaway is that the simulated groundwater velocity field must replicate that of the complete GHE to accurately capture pairwise thermal interactions and enable spatial superposition. Further research is therefore needed to adapt the two-SCW methodology to properly capture the asymmetric advective effects that develop under bleed conditions.

4. Conclusion

This study builds on the method proposed by Rose et al. [27] to construct transfer functions for fields of standing column wells (SCW) operating under bleed conditions. The approach uses numerically simulated hydraulic and thermal interactions between SCWs to construct transfer functions under uniform inlet temperature boundary conditions. The methodology is verified against a reference 3D numerical model under various flow rate scenarios. Results show that, in the absence of bleed, modelling only two SCWs at a time accurately reproduces the reference transfer functions. However, when bleed is activated, this configuration introduces discrepancies arising from an inaccurate representation of the groundwater velocity field, leading to an underestimation of advective heat transfer. It was demonstrated that the groundwater velocity field generated by the pumping of every SCW in the ground heat exchanger must be used to correctly capture pairwise thermal interactions. Future work should focus on developing a more efficient and memory-light modelling strategy capable of accurately representing both hydraulic and thermal interactions without requiring full-scale simulation of the entire ground heat exchanger.

Nomenclature

Symbols

β	Bleed ratio [–]	ϕ	Diameter [m]
ρ	Density [kgm^{-3}]	ΔT	Temperature difference [K]
Γ	Boundary condition [–]	Ω	Domain [–]
A	Cross-sectional area [m^2]	b	Thickness [m]
$\dot{B}$	Bleed flow rate [m^3s^{-1}]	c	Specific heat capacity [$Jkg^{-1}K^{-1}$]
h	Hydraulic head [m]	H	Height [m]
k	Thermal conductivity [$Wm^{-1}K^{-1}$]	K	Hydraulic conductivity [ms^{-1}]

n	Porosity [–]	r	Radius [m]
s	Drawdown [m]	S_s	Specific storage [m^{-1}]
t	Time [s]	T	Temperature [K]
$\dot{V}$	Pumping flow rate [m^{3}s^{-1}]	x, y, z	Coordinates [m]
$\boldsymbol{g}$	Transfer function [–]	$\boldsymbol{n}$	Vector perpendicular to a boundary [–]
$\boldsymbol{q}$	Conductive heat flux vector [Wm^{-2}]	$\boldsymbol{q_c}$	Convective heat flux vector [Wm^{-2}]
$\boldsymbol{u}$	Fluid flow vector [ms^{-1}]		

Subscripts

D	Darcy	eq	Equivalent
f	Fluid phase	ij	Mutual interaction
in	Inlet or Inner	out	Outlet or Outer
p	Pipe material	s	Solid phase
w	Groundwater		

Abbreviations

FEM	Finite element model	GHE	Ground heat exchanger
MaxRe	Maximum relative error	RRMSE	Relative root mean square error
SCW	Standing column well		

Acknowledgements

The authors acknowledge the support from partners of the Geothermal Research Chair on the Integration of SCWs in Institutional Buildings, namely Hydro-Québec, the Ministry of higher education of Québec, CSSMI, CSSDM, CSSS, Versa Profiles, Marmott Energies, CanmetEnergy and NSERC. Additionally, we thank the anonymous reviewers and colleagues that provided constructive comments. This work was financed by the Natural Sciences and Engineering Research Council of Canada, Canada through grant number ALLRP 544477-19.

References

[1] Ma Z, Xia L, Gong X, Kokogiannakis G, Wang S, Zhou X. Recent advances and development in optimal design and control of ground source heat pump systems. *Renewable and Sustainable Energy Reviews* 2020;**131**:110001.

[2] O'Neill ZD, Spitler JD, Rees SJ. Performance Analysis of Standing Column Well Ground Heat Exchanger Systems. *ASHRAE Transactions* 2006;**112**(6):633–43.

[3] Beaudry G, Faucher J, Tonellato G, Pasquier P, Kummert M., 2024. "Standing column wells in cold climates: lessons learned after one year of operating a demonstration system in Canada," Proceedings of the IGSHPA Research Track 2024. Montréal, Canada. p. 259–68.

[4] Dion G, Philippe P., 2025. "Adaptation of sizing equations for standing column wells," Proceedings of the European Geothermal Congress 2025. Zurich, Switzerland. p. 1–8.

[5] Kim D, Lim M, Yu B, Lee C. Smart Heating and Cooling Heat Pump System by Standing Column Well and Cross-Mixing Balancing Well Heat Exchangers. *Applied Sciences* 2020;**10**(21):7643.

[6] Jacques L, Pasquier P, Dion G, Beaudry G. Experimental assessment of inter-well reinjection in standing column wells by analysis of transfer functions obtained from non-stationary deconvolution. *Geothermics* 2025;**125**:103184.

[7] Spitler JD, Rees SJ, Deng Z, Chiasson A, Orio CD, Johnson C. R&D studies applied to standing column well design. *Technical Report ASHRAE 1119-RP* 2002;1–123.

[8] Pasquier P, Nguyen A, Eppner F, Marcotte D, Baudron P. 10 - Standing column wells. In: Rees SJ, editor. *Advances in Ground-Source Heat Pump Systems*, Woodhead Publishing; 2016, p. 269–94.

[9] Laroche V, Pasquier P, Courcelles B. Integration of standing column wells in urban context: A numerical investigation-case in the City of Montreal. *Sustainable Cities and Society* 2022;**78**:103513.

[10] Faucher J. *Décarbonation des bâtiments existants avec des pompes à chaleur géothermiques haute température*. Master thesis. Polytechnique Montréal; 2025.

[11] Ahmadfard M, Bernier M. Modifications to ASHRAE's sizing method for vertical ground heat exchangers. *Science and Technology for the Built Environment* 2018;**24**(7):803–17.

[12] Nguyen A, Pasquier P, Marcotte D. Thermal resistance and capacity model for standing column wells operating under a bleed control. *Renewable Energy* 2015;**76**:743–56.

[13] Beurcq C. *Control Strategies for Standing Column Wells in a Cold Climate*. Master thesis. Polytechnique Montréal; 2019.

[14] Beaudry G, Pasquier P, Marcotte D, Zarrella A. Flow rate control in standing column wells: A flexible solution for reducing the energy use and peak power demand of the built environment. *Applied Energy* 2022;**313**:118774.

[15] Beaudry G, Pasquier P, Marcotte D. A fast convolution-based method to simulate time-varying flow rates in closed-loop and standing column well ground heat exchangers. *Renewable Energy* 2021;**174**:55–72.

[16] Beaudry G, Pasquier P, Nguyen A. New formulations and experimental validation of non-stationary convolutions for the fast simulation of time-variant flowrates in ground heat exchangers. *Science and Technology for the Built Environment* 2023;**30**:208–19.

[17] Eskilson P. *Thermal analysis of heat extraction boreholes*. Doctoral thesis. University of Lund; 1987.

[18] Pasquier P, Marcotte D. Joint use of quasi-3D response model and spectral method to simulate borehole heat exchanger. *Geothermics* 2014;**51**:281–99.

[19] Cimmino M. The effects of borehole thermal resistances and fluid flow rate on the g-functions of geothermal bore fields. *International Journal of Heat and Mass Transfer* 2015;**91**:1119–27.

[20] Cimmino M, Bernier M, Adams F. A contribution towards the determination of g-functions using the finite line source. *Applied Thermal Engineering* 2013;**51**(1):401–12.

[21] Ng BM, Underwood CP, Walker SL. Standing column wells – Modeling the potential for applications in geothermal heating and cooling. *HVAC&R Research* 2011;**17**(6):1089–100.

[22] Beaudry G, Pasquier P, Marcotte D. The impact of rock fracturing and pump intake location on the thermal recovery of a standing column well: model development, experimental validation, and numerical analysis. *Science and Technology for the Built Environment* 2019;**25**(8):1052–68.

[23] Robert S, Pasquier P, Nguyen A. Impact of layered heterogeneity on thermal response test interpretation performed on a standing column well operated without bleed. *Geothermics* 2022;**101**:102353.

[24] Nguyen A, Jacques L, Pasquier P. An easy-to-use analytical model for standing column wells operating with bleed. *Applied Thermal Engineering* 2025;**258**:124543.

[25] Jacques L, Pasquier P, Nguyen A, Beaudry G. Improvement and experimental validation of an analytical model for standing column wells operated with bleed. *Applied Thermal Engineering* 2025;**279**:127620.

[26] Rose C, Pasquier P, Nguyen A, Labib R., 2025. "Approximation of short-term transfer functions for standing column well heat exchangers using wavelet decomposition and artificial neural networks," Proceedings of the European Geothermal Congress 2025. Zurich, Switzerland. p. 1–10.

[27] Rose C, Pasquier P, Nguyen A, Labib R. A unified framework for the construction of short- and long-term g-functions for parallel-connected ground heat exchangers. *International Journal of Heat and Mass Transfer 2026;***261***:*128565.

[28] Dusseault B, Pasquier P, Marcotte D. A block matrix formulation for efficient g-function construction. *Renewable Energy* 2018;**121**:249–60.

[29] Nguyen A, Pasquier P. A successive flux estimation method for rapid g-function construction of small to large-scale ground heat exchanger. *Renewable Energy* 2021;**165**:359–68.

[30] Theis CV. The relation between the lowering of the Piezometric surface and the rate and duration of discharge of a well using ground-water storage. *Eos, Transactions American Geophysical Union* 1935;**16**(2):519-24.

[31] Pasquier P, Marcotte D. Efficient computation of heat flux signals to ensure the reproduction of prescribed temperatures at several interacting heat sources. *Applied Thermal Engineering* 2013;**59**(1):515–26.

[32] Marcotte D, Pasquier P. Unit-response function for ground heat exchanger with parallel, series or mixed borehole arrangement. *Renewable Energy* 2014;**68**:14–24.

[33] Champagne-Péladeau L, Pasquier P, Millette D, Dupuis JC. Delineation of the thermal plume associated with a standing column well system in a fractured aquifer using numerical modeling. *Geothermics* 2025;**127**:103260.